# Nucleon and nucleon-pair correlations in $A \leq 12$ nuclei

Robert B. Wiringa, Physics Division, Argonne National Laboratory

Joe Carlson, Los Alamos
Stefano Gandolfi, Los Alamos
Diego Lonardonit, Michigan State
Alessandro Lovato, Argonne
Saori Pastore, Washington U. St.louis
Maria Piarulli, Washington U. St.louis
Steve Pieper, Argonne
Rocco Schiavilla, JLab & ODU

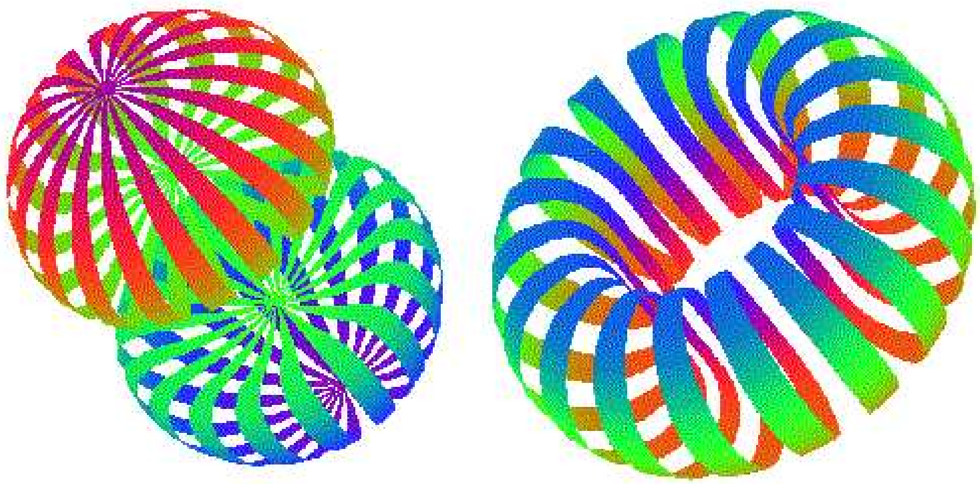

WORK NOT POSSIBLE WITHOUT EXTENSIVE COMPUTER RESOURCES

Argonne Laboratory Computing Resource Center (Bebop)

Argonne Leadership Computing Facility (Theta)

Argonne NATIONAL LABORATORY

Physics Division

Work supported by U.S. Department of Energy, Office of Nuclear Physics

# NUCLEAR HAMILTONIAN


$$H = \sum_i K_i + \sum_{i<j} v_{ij} + \sum_{i<j<k} V_{ijk}$$

$K_i$: Non-relativistic kinetic energy, $m_n$-$m_p$ effects included

Argonne v$_{18}$: $v_{ij} = v^{\gamma}_{ij} + v^{\pi}_{ij} + v^{I}_{ij} + v^{S}_{ij} = \sum v_p(r_{ij}) O^p_{ij}$

- 18 spin, tensor, spin-orbit, isospin, etc., operators
- full EM and strong CD and CSB terms included
- predominantly local operator structure
- fits Nijmegen PWA93 data with $\chi^2$/d.o.f.=1.1

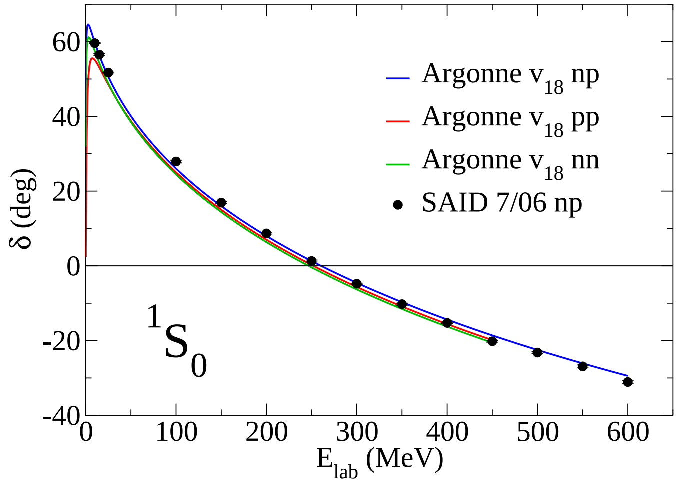


Wiringa, Stoks, & Schiavilla, PRC **51**, (1995)

Urbana & Illinois: $V_{ijk} = V^{2\pi}_{ijk} + V^{3\pi}_{ijk} + V^{R}_{ijk}$

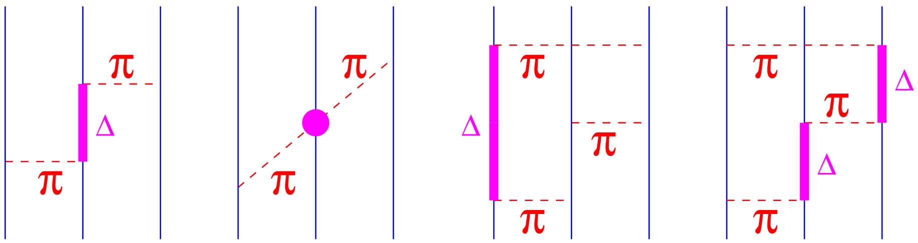


- Urbana has standard $2\pi$ $P$-wave + short-range repulsion for matter saturation
- Illinois adds $2\pi$ $S$-wave + $3\pi$ rings to provide extra $T$=3/2 interaction
- Illinois-7 has four parameters fit to 23 levels in $A \leq$10 nuclei

Pieper, Pandharipande, Wiringa, & Carlson, PRC **64**, 014001 (2001)
Pieper, AIP CP **1011**, 143 (2008)

Norfolk NV2: $v_{ij} = v_{ij}^{\gamma} + v_{ij}^{\pi} + v_{ij}^{2\pi} + v_{ij}^{CT} = \sum v_p(r_{ij}) O_{ij}^p$

- derived in chiral effective field theory with $\Delta$-intermediate states
- 17 spin, tensor, spin-orbit, isospin, etc., operators
- full EM and strong CD and CSB terms included
- predominantly local operator structure suitable for quantum Monte Carlo
- multiple models with different regularization fit to Granada PWA2013 data
- Ia,b,c fit to $E_{\rm lab}$ = 125 MeV with $\chi^2$/d.o.f.$\sim$1.1
- IIa,b,c fit to $E_{\rm lab}$ = 200 MeV with $\chi^2$/d.o.f.$\sim$1.4

Piarulli, Girlanda, Schiavilla, Kievsky, Lovato, Marcucci, Pieper, Viviani, & Wiringa, PRC **94**, 054007 (2016)

Norfolk NV3: $V_{ijk} = V_{ijk}^{2\pi} + V_{ijk}^{CT}$

- standard $2\pi$ $S$-wave and $2\pi$ $P$-wave terms consistent with chiral $NN$ potential
- contact terms of $c_D$ ($\pi$-short range) and $c_E$ (short-short range $\tau_i \cdot \tau_k$) type
- two parameters fit to $^3$H binding and $nd$ scattering length

Piarulli, Baroni, Girlanda, Kievsky, Lovato, Marcucci, Pieper, Schiavilla, Viviani, & Wiringa, PRL **120**, 052503 (2018)

# VARIATIONAL MONTE CARLO

Minimize expectation value of $H$

$$E_V = \frac{\langle \Psi_V | H | \Psi_V \rangle}{\langle \Psi_V | \Psi_V \rangle} \geq E_0$$

using Metropolis Monte Carlo and trial function

$$|\Psi_V\rangle = \left[ \mathcal{S} \prod_{i<j} (1 + U_{ij} + \sum_{k \neq i,j} U_{ijk}) \right] \left[ \prod_{i<j} f_c(r_{ij}) \right] |\Phi_A(JMTT_3)\rangle$$

- single-particle $\Phi_A(JMTT_3)$ is fully antisymmetric and translationally invariant
- central pair correlations $f_c(r)$ keep nucleons at favorable pair separation
- pair correlation operators $U_{ij} = \sum_p u_p(r_{ij}) O^p_{ij}$ reflect influence of $v_{ij}$
- triple correlation operator $U_{ijk}$ added when $V_{ijk}$ is present
- multiple $J^\pi$ states constructed and diagonalized for p-shell nuclei
- ability to construct clusterized or asymptotically correct trial functions
- optimization code COBYLA used to search parameters

$\Psi_V$ are spin-isospin vectors in $3A$ dimensions with $\sim 2^A \binom{A}{Z}$ components


Lomnitz-Adler, Pandharipande, & Smith, NP **A361**, 399 (1981)
Wiringa, PRC **43**, 1585 (1991)

# Green's Function Monte Carlo

Projects out lowest energy state from variational trial function

$$\Psi(\tau) = \exp[-(H - E_0)\tau]\Psi_V = \sum_n \exp[-(E_n - E_0)\tau]a_n\psi_n$$

$$\Psi(\tau \to \infty) = a_0\psi_0$$

Evaluation of $\Psi(\tau)$ done stochastically in small time steps $\Delta\tau$

$$\Psi(\mathbf{R}_n, \tau) = \int G(\mathbf{R}_n, \mathbf{R}_{n-1}) \cdots G(\mathbf{R}_1, \mathbf{R}_0)\Psi_V(\mathbf{R}_0) d\mathbf{R}_{n-1} \cdots d\mathbf{R}_0$$

Mixed estimates used for expectation values; $\Psi(\tau) = \Psi_V + \delta\psi(\tau)$ and neglect $O(\delta\psi(\tau)^2)$

$$\langle O(\tau)\rangle = \frac{\langle\Psi(\tau)|O|\Psi(\tau)\rangle}{\langle\Psi(\tau)|\Psi(\tau)\rangle} \approx \langle O(\tau)\rangle_{\text{Mixed}} + [\langle O(\tau)\rangle_{\text{Mixed}} - \langle O\rangle_V]$$

$$\langle O(\tau)\rangle_{\text{Mixed}} = \frac{\langle\Psi_V|O|\Psi(\tau)\rangle}{\langle\Psi_V|\Psi(\tau)\rangle} \quad ; \quad \langle H(\tau)\rangle_{\text{Mixed}} = \frac{\langle\Psi(\tau/2)|H|\Psi(\tau/2)\rangle}{\langle\Psi(\tau/2)|\Psi(\tau/2)\rangle} \geq E_0$$

- Cannot propagate $p^2$, $L^2$, or $(\mathbf{L}\cdot\mathbf{S})^2$ operators $\Rightarrow$ use $H'$ = AV8′ + $\tilde{V}_{ijk}$
- Fermion sign problem would limit maximum $\tau$, but ...
- Constrained-path propagation removes steps that have $\overline{\Psi^\dagger(\tau, \mathbf{R})\Psi_V(\mathbf{R})} = 0$
- Multiple excited states of same $J^\pi$ stay orthogonal


Carlson, PRC **38**, 1879 (1988)

Pudliner, Pandharipande, Carlson, Pieper, & Wiringa, PRC **56**, 1720 (1997)

Wiringa, Pieper, Carlson, & Pandharipande, PRC **62**, 014001 (2000)

Carlson, Gandolfi, Pederiva, Pieper, Schiavilla, Schmidt, & Wiringa, RMP **87**, 1067 (2015)

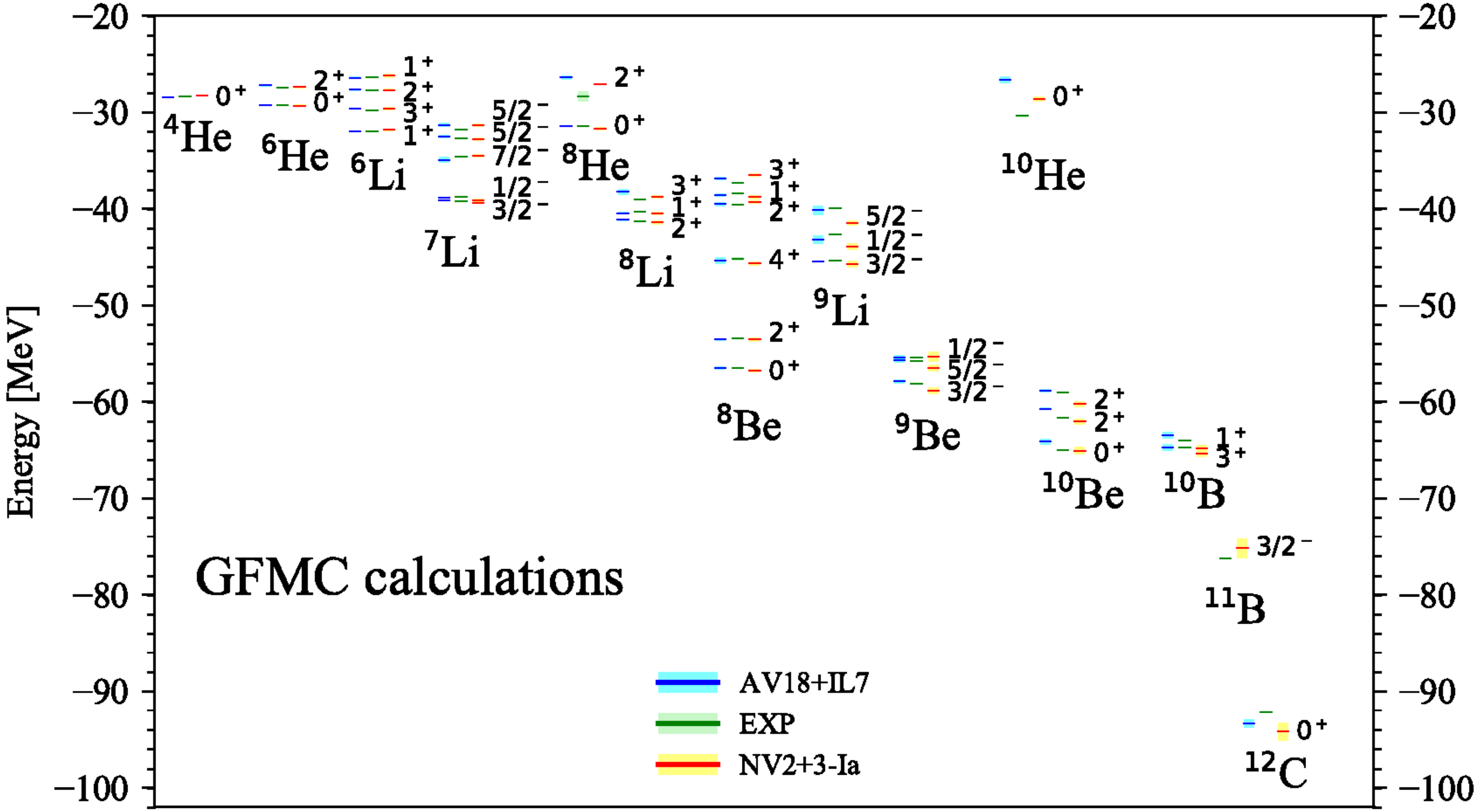


RMS $\Delta E$ for 36 states: AV18+IL7 = 0.80 MeV ; NV2+3-Ia = 0.72 MeV

with signed average deviation: -0.23 MeV and +0.15 MeV

# Single-Nucleon Momentum Distributions

Momentum distributions of nucleons and nucleon clusters can provide useful insights into various reactions on nuclei, such as $(e,e'p)$ and $(e,e'pN)$ electrodisintegration processes.

Probability of finding a nucleon in a nucleus with momentum $\mathbf{k}$ in a given spin-isospin state:

$$\rho_{\sigma\tau}(\mathbf{k}) = \int d\mathbf{r}'_1 d\mathbf{r}_1 d\mathbf{r}_2 \cdots d\mathbf{r}_A \, \psi^\dagger_{JM_J}(\mathbf{r}'_1, \mathbf{r}_2, \ldots, \mathbf{r}_A) \, e^{-i\mathbf{k}\cdot(\mathbf{r}_1 - \mathbf{r}'_1)} \, P_{\sigma\tau}(1) \, \psi_{JM_J}(\mathbf{r}_1, \mathbf{r}_2, \ldots, \mathbf{r}_A)$$

where $P_{\sigma\tau}$ is a spin-isospin projection operator and the normalization is:

$$N_{\sigma\tau} = \int \frac{d\mathbf{k}}{(2\pi)^3} \, \rho_{\sigma\tau}(\mathbf{k})$$

$N_{\sigma\tau}$ is the total number of nucleons with given spin-isospin.

Compute the Fourier transform by Metropolis Monte Carlo integration, using a standard Metropolis walk, guided by $|\Psi_{JM_J}(\mathbf{r}_1, \ldots, \mathbf{r}_i, \ldots, \mathbf{r}_A)|^2$ to sample configurations. Average over all particles $i$ in each configuration; for each particle use a grid of Gauss-Legendre points $\mathbf{x}_i$ in a randomly chosen direction and move positions in both left- and right-hand side wave functions symmetrically away from their central value:

$$\rho_{\sigma\tau}(\mathbf{k}) = \frac{1}{A} \sum_i \int d\mathbf{r}_1 \cdots d\mathbf{r}_i \cdots d\mathbf{r}_A \int d\mathbf{\Omega}_x \int_0^{x_{\max}} x^2 dx \, \psi^\dagger_{JM_J}(\mathbf{r}_1, \ldots, \mathbf{r}_i + \mathbf{x}/2, \ldots, \mathbf{r}_A)$$

$$e^{-i\mathbf{k}\cdot\mathbf{x}} \, P_{\sigma\tau}(i) \, \psi_{JM_J}(\mathbf{r}_1, \ldots, \mathbf{r}_i - \mathbf{x}/2, \ldots, \mathbf{r}_A)$$

Deuteron proton momentum distribution has contributions from the $S$- and $D$-wave components of the wave function; $S$-wave has node at 2 $\mathrm{fm}^{-1}$ that $D$-wave fills in to give a broad high-momentum shoulder out to $> 7\ \mathrm{fm}^{-1}$ before the second $S$-wave and first $D$-wave node.

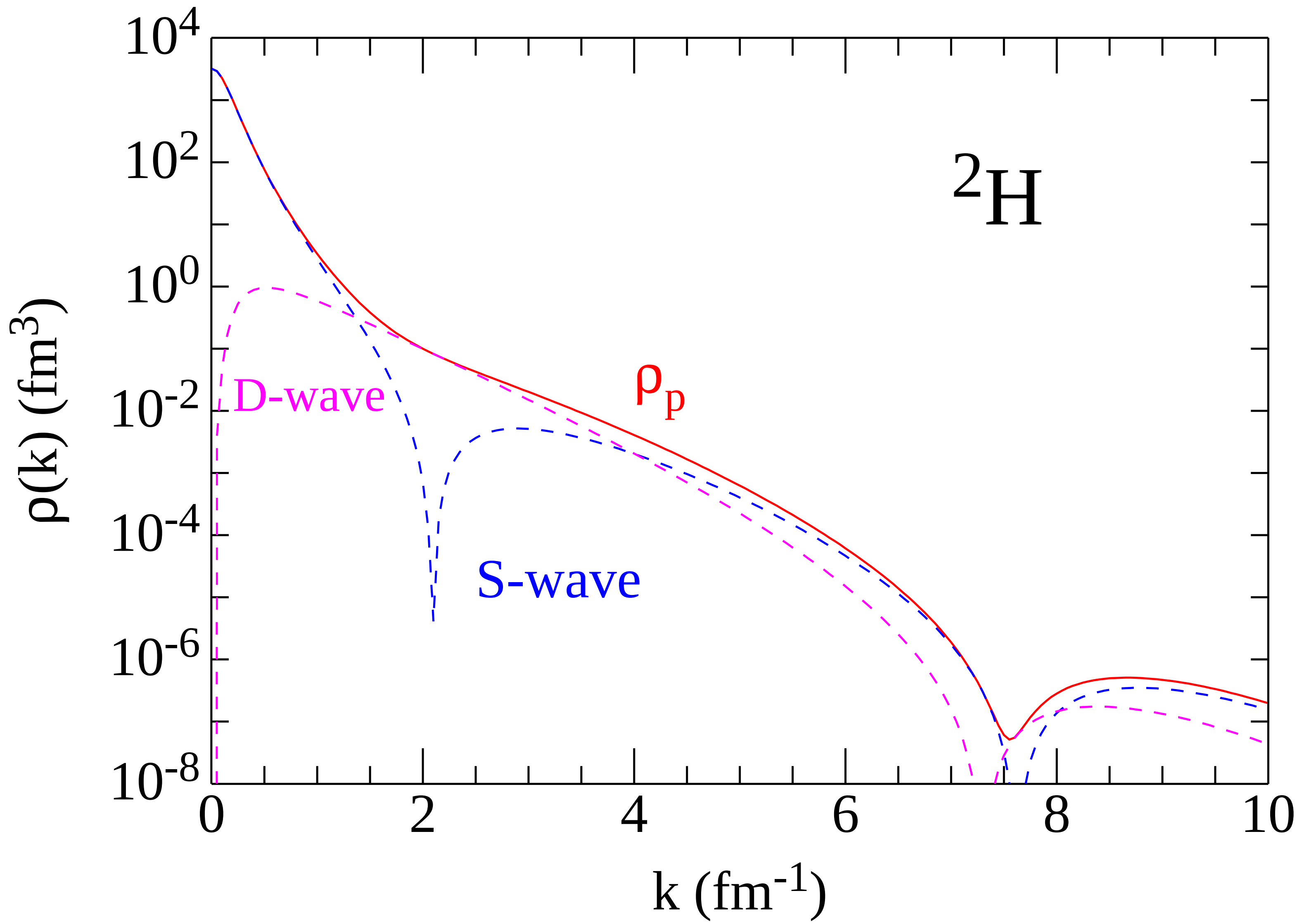

Compare the relatively “hard” AV18 deuteron with the Norfolk NV2 $\chi$EFT potentials:

NV2-Ia “soft” cutoff fit to $E_{lab}$=125 MeV (solid) ; NV2-Ib “hard” cutoff (dashed)

NV2-IIa “soft” cutoff fit to $E_{lab}$=200 MeV (dashed) ; NV2-IIb “hard” cutoff (solid)

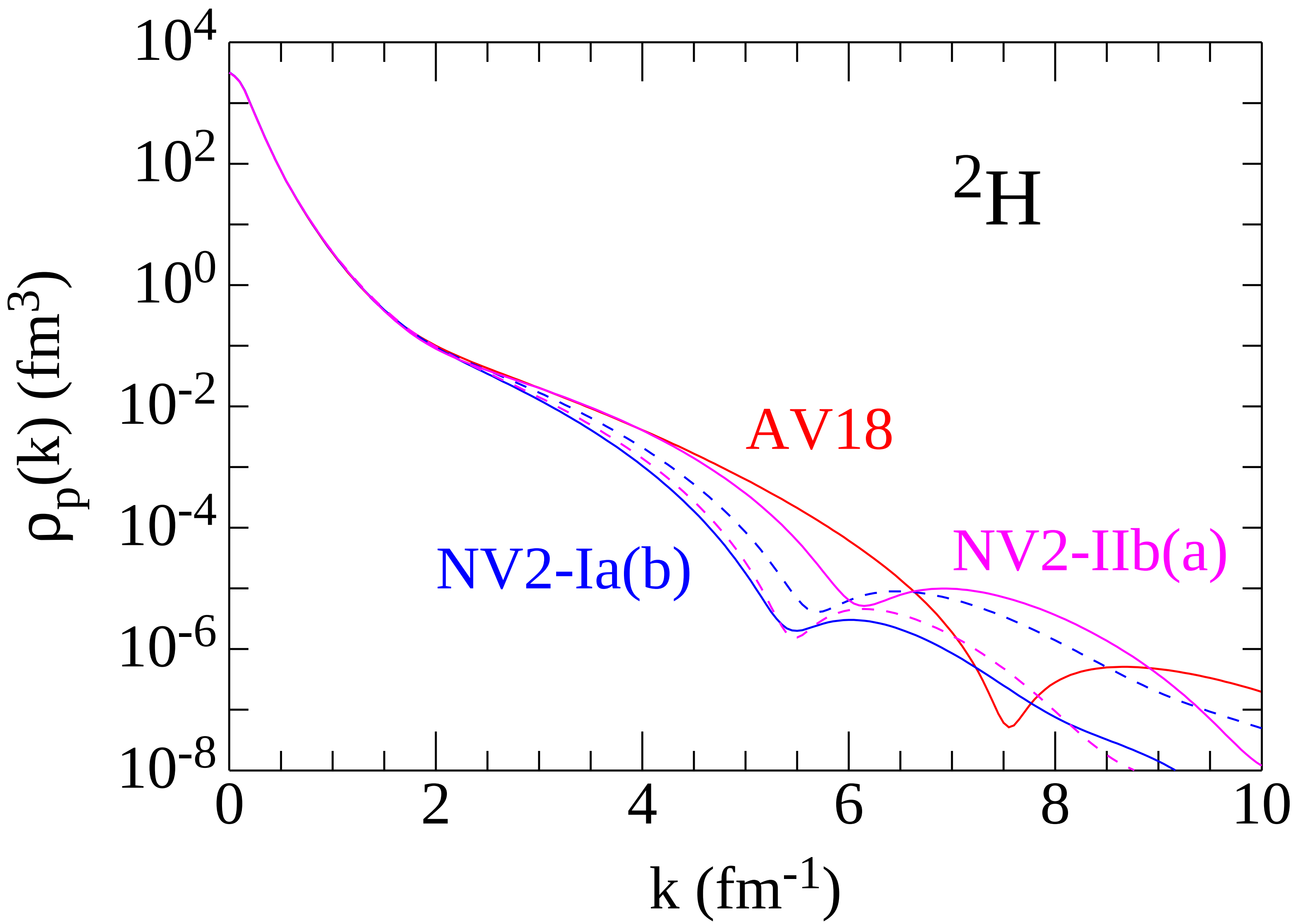

$^3$He in the $M_J = \frac{1}{2}^+$ state has spin-up proton and neutron distributions very similar to the deuteron, while the spin-down proton distribution is slightly larger, particularly in the dip region; the spin-down neutron distribution has a typical $D$-wave shape and is present due to the 9% $D$-state in the trinucleon wave function.

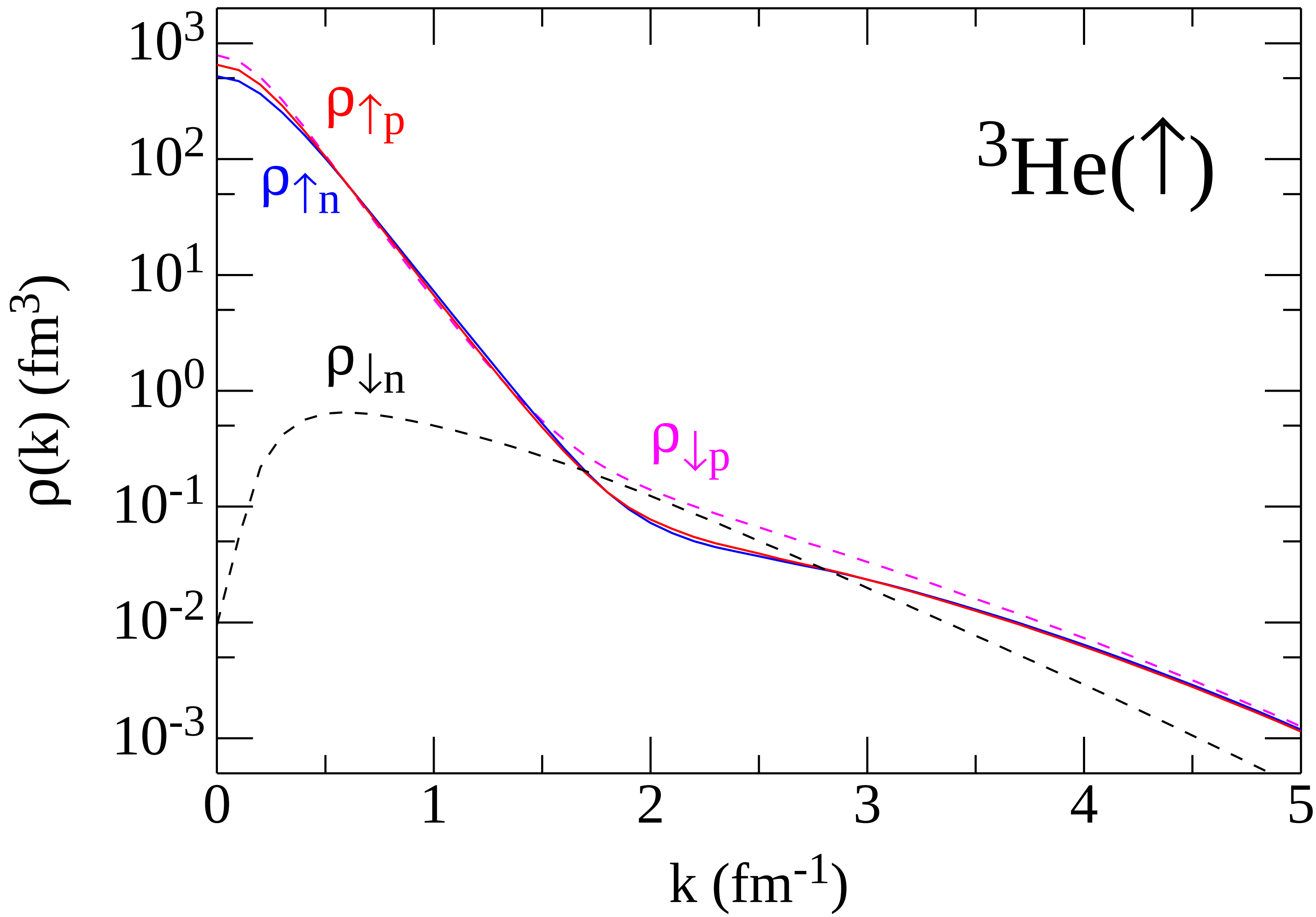

$^4$He proton momentum distribution is very similar to the deuteron, but is smaller at $k = 0$ and greater in the high-momentum shoulder because of the greater binding energy. Also shown are the nucleon cluster momentum distributions for $tp$ and $dd$ partitions.

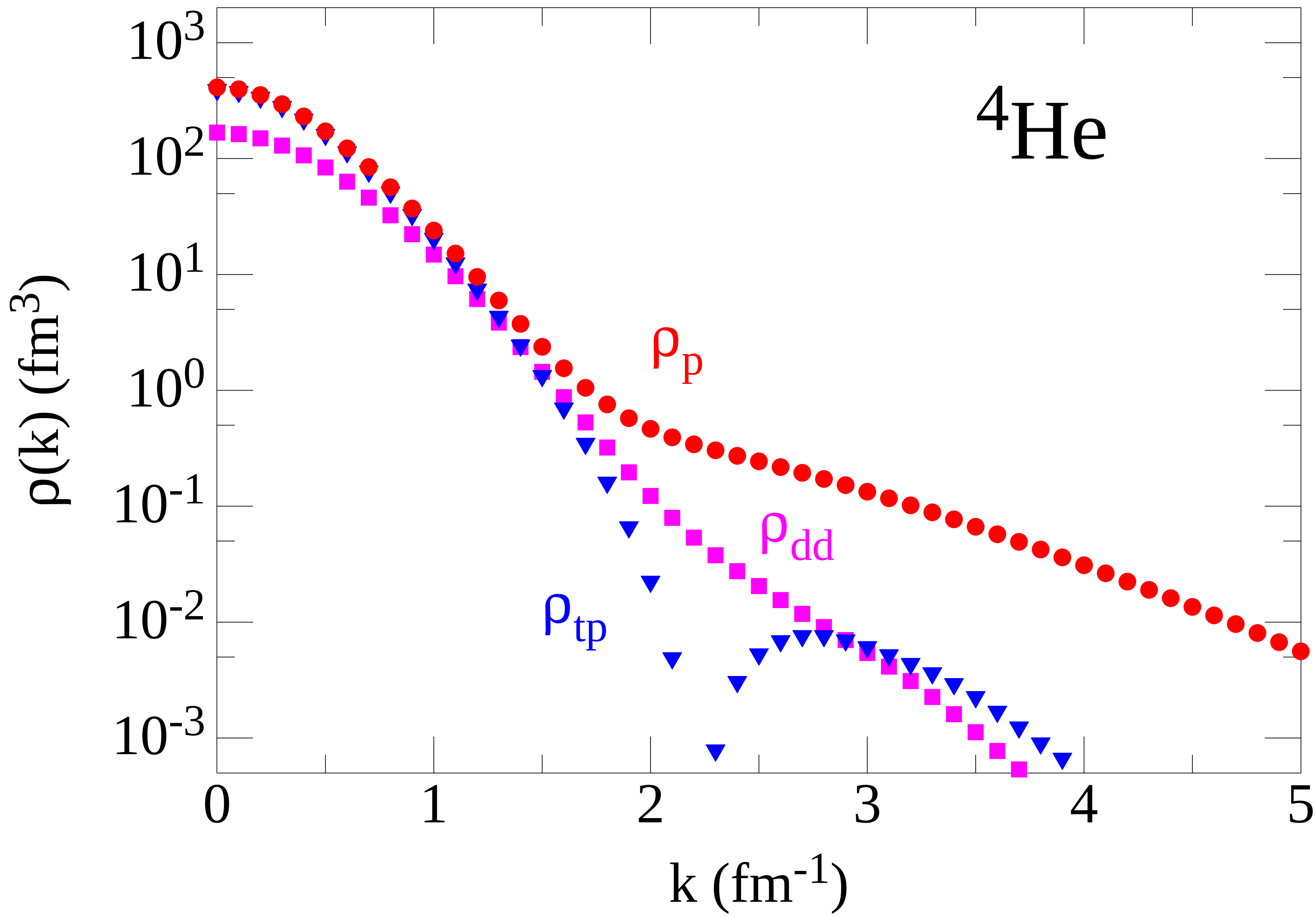

To study source of higher momentum densities, we show calculations for AV18+UX, for AV18 alone, for AV18(4) with tensor correlations removed, and for AV18(J) with only cental Jastrow correlations. The numbers of protons above $k = 1.4\ \mathrm{fm}^{-1}$ (out of 2 total) for these cases are 0.25, 0.20, 0.10, and 0.05, respectively.

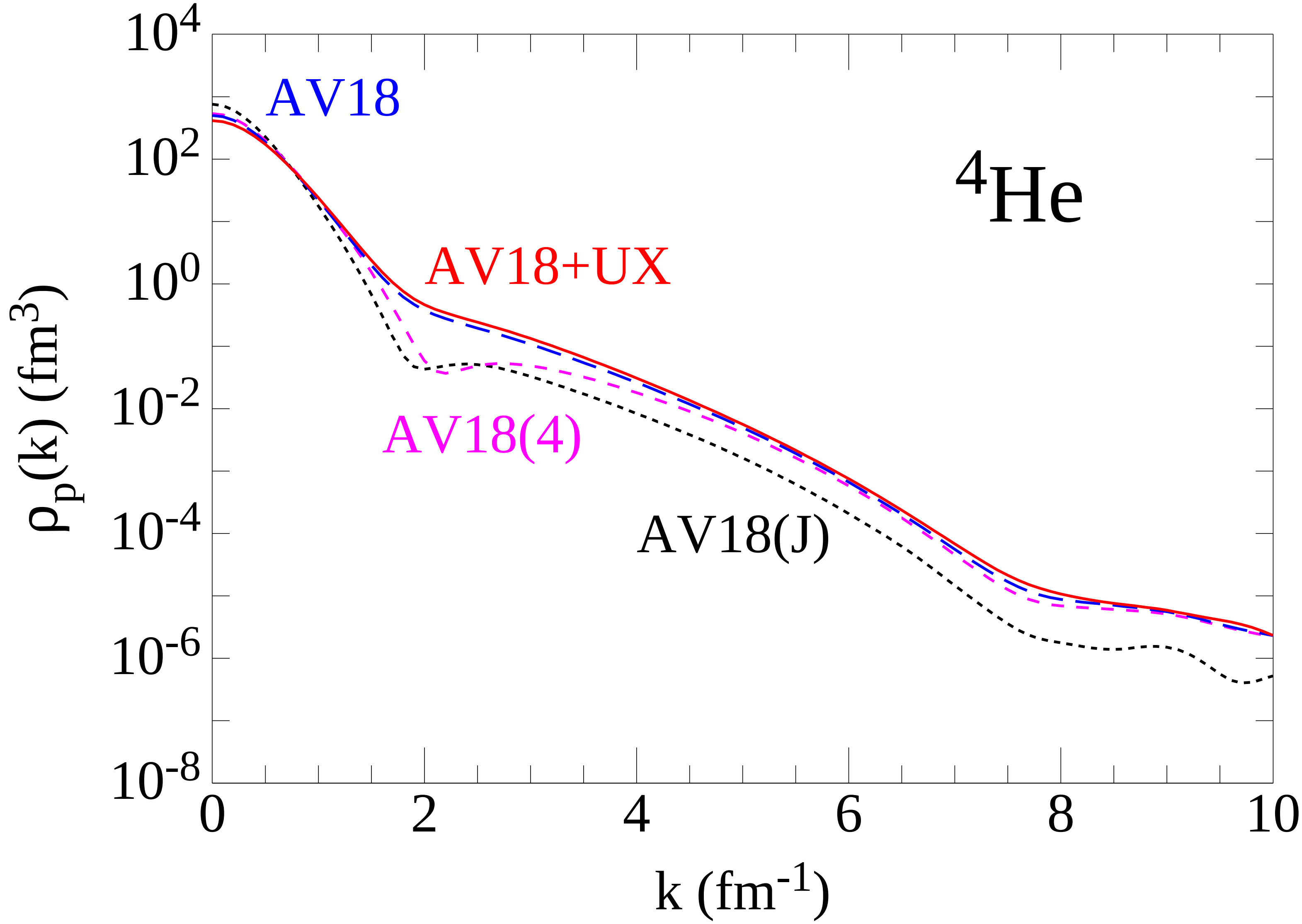

Compare the relatively "hard" AV18+UX $^4$He with the Norfolk NV2+3 $\chi$EFT potentials:

NV2+3-Ia "soft" cutoff fit to $E_{lab}$=125 MeV (solid) ; NV2+3-Ib "hard" cutoff (dashed)

NV2+3-IIa "soft" cutoff fit to $E_{lab}$=200 MeV (dashed) ; NV2+3-IIb "hard" cutoff (solid)

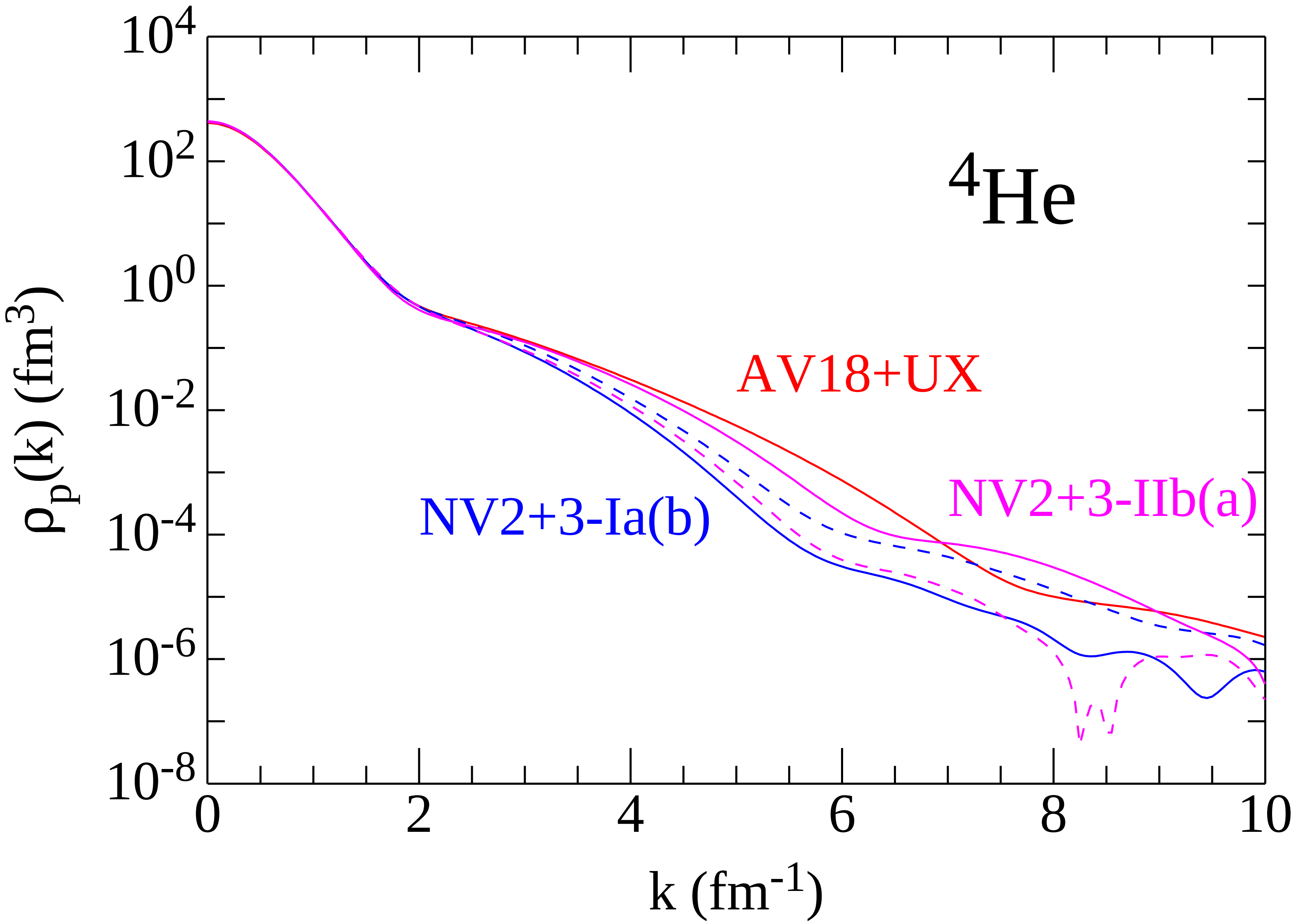

$^6$He proton momentum distribution is very similar to $^4$He, while neutron distribution peaks at $k > 0$ because of added $p$-shell neutrons; $(\rho_n - \rho_p)$ difference approximates the halo neutron distribution, where the two neutrons are primarily in a relative $S$-wave with corresponding dip.

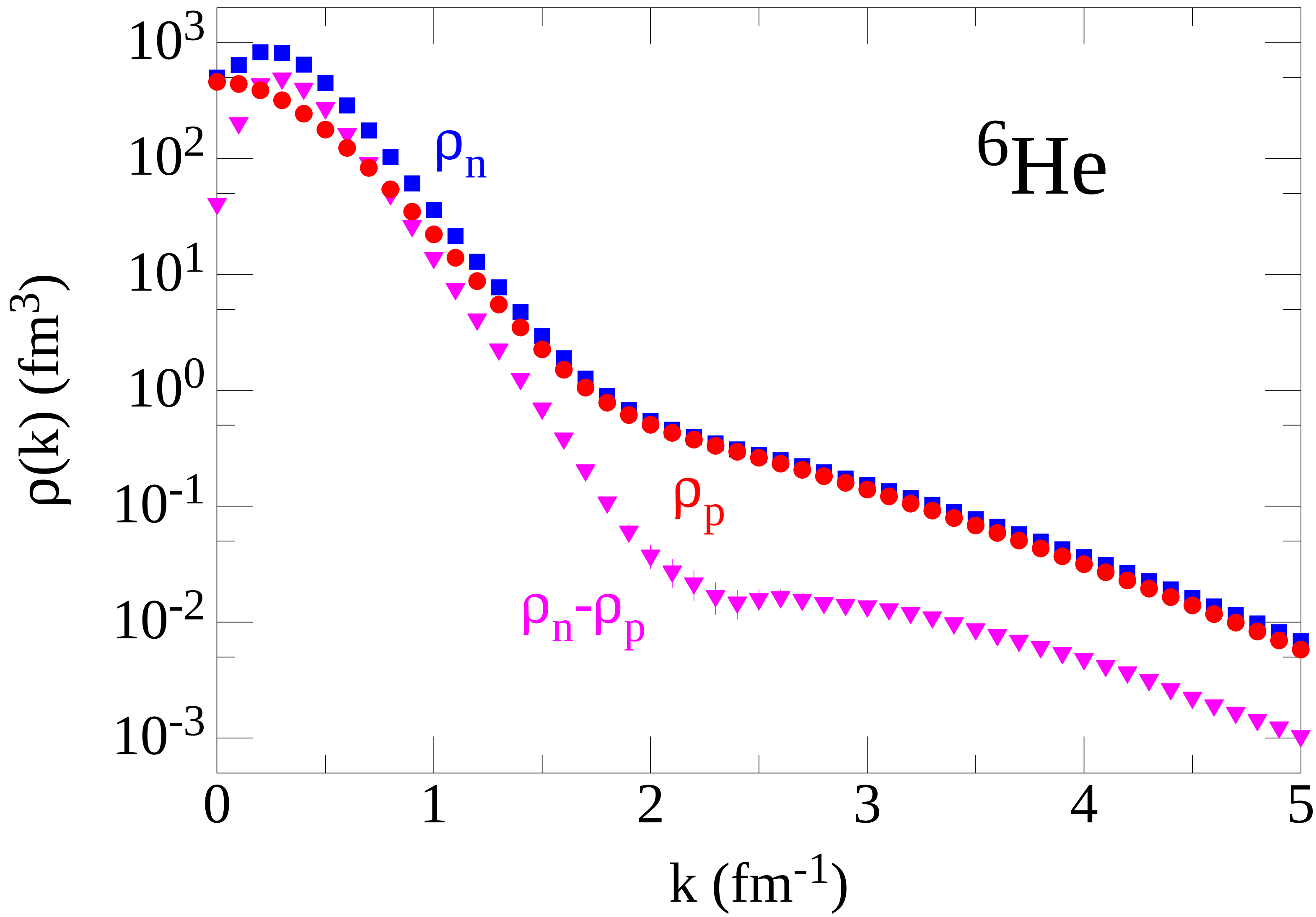

$^6$Li total nucleon momentum distribution $\rho_N = \rho_p + \rho_n$ has the same overall shape, with slightly broadened low-momentum region that is sum of $s$- and $p$-shell nucleons. The $\alpha$-$d$ cluster distribution in the $1^+$ ground state is almost identical at zero momentum with a node at 0.7 fm$^{-1}$ because of antisymmetry - a node not present in the $3^+$ first excited state.

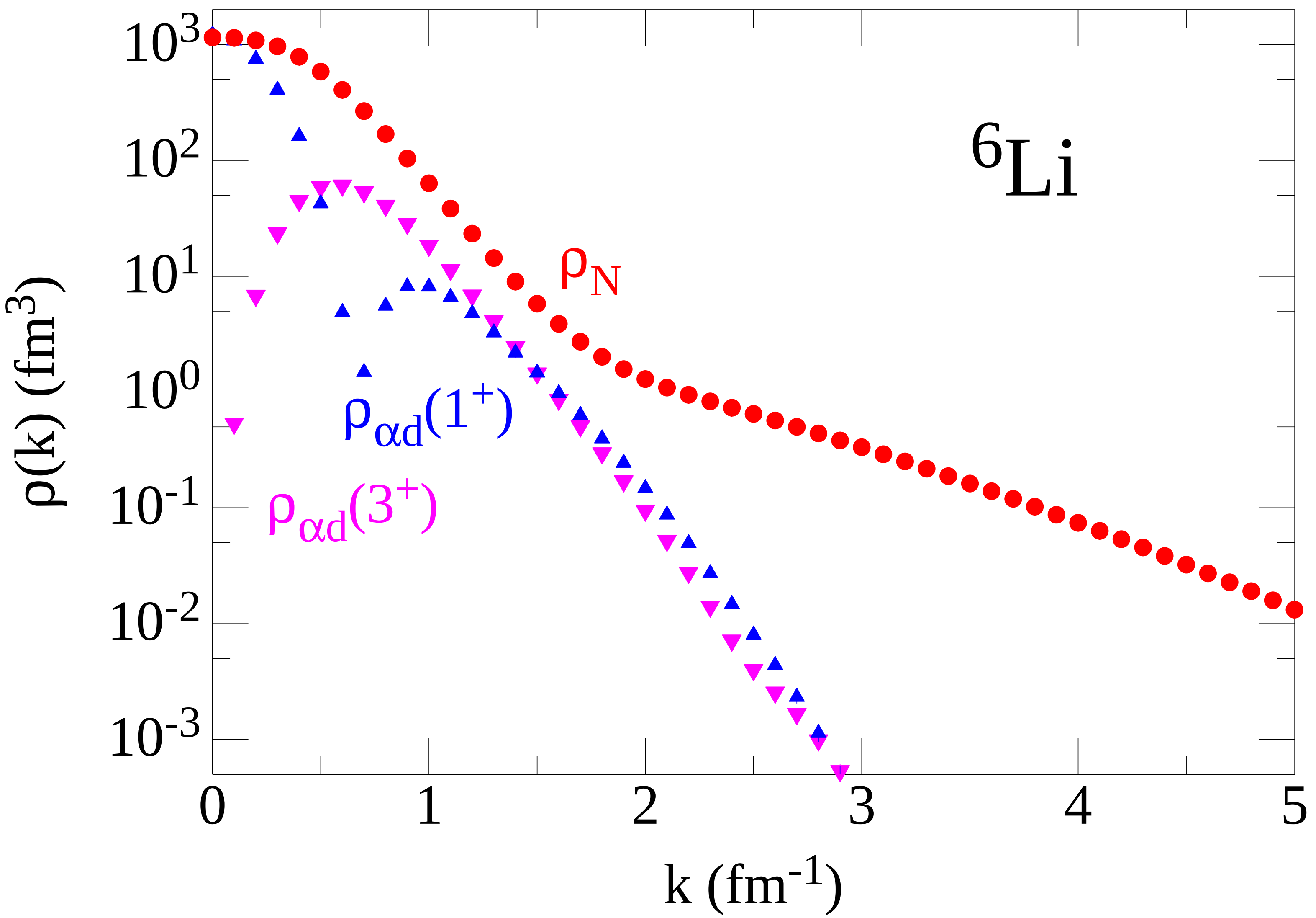

$^7$Li momentum distributions follow the same general pattern; the $\alpha t$ cluster distribution for the $^3/_2^-$ ground state (and $^1/_2^-$ first excited state) has nodes at k=0 and 1.2 fm$^{-1}$ because of parity and antisymmetry, while the $^7/_2^-$ second (and $^5/_2^-$ third) excited state has only the node at k=0.

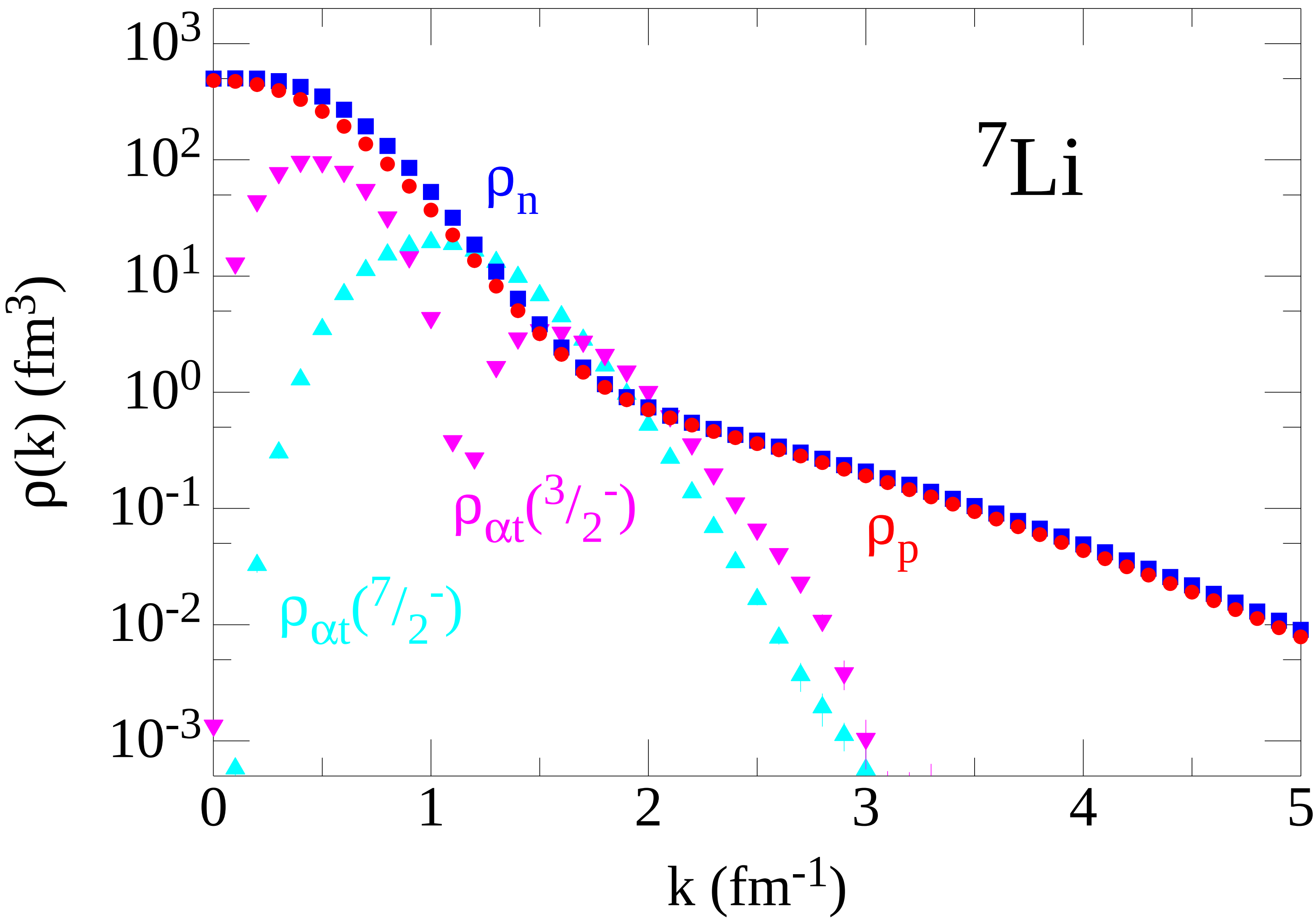

$^8$Be proton momentum distributions follow the same general pattern; the $\alpha\alpha$ cluster distribution in the $0^+$ ground state is in a $2s$ spatial distribution because of parity and antisymmetry and at $k = 0$ the two distributions are equal; for the $2^+$ first excited state the shape is $1d$.

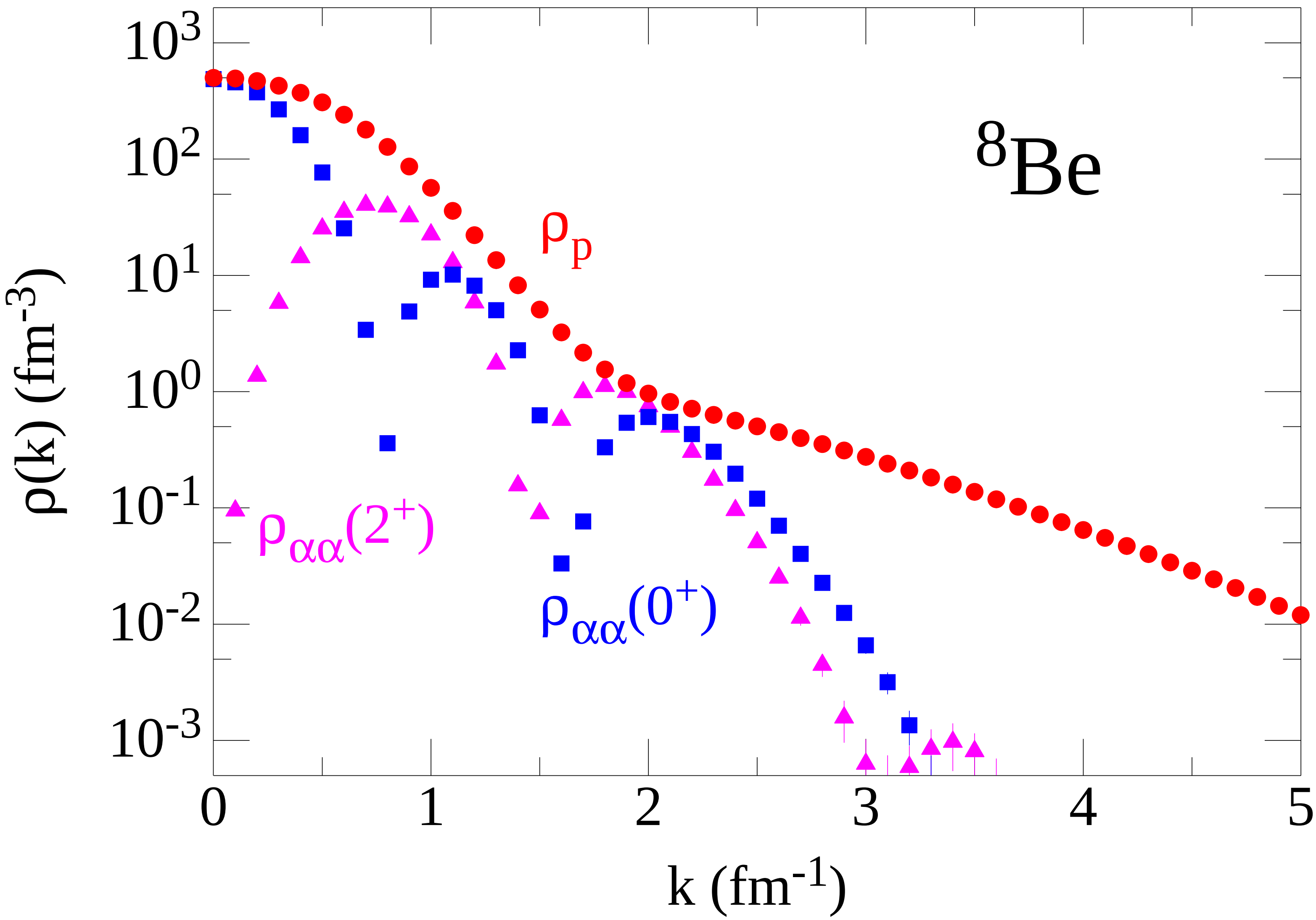

The proton momentum distributions in $T = 0$ light nuclei all have similar shapes, with the $k = 0$ peak decreasing in magnitude and broadening out as the binding increases and $p$-shell nucleons are added. The high momentum shoulder due to pion-exchange is universal.

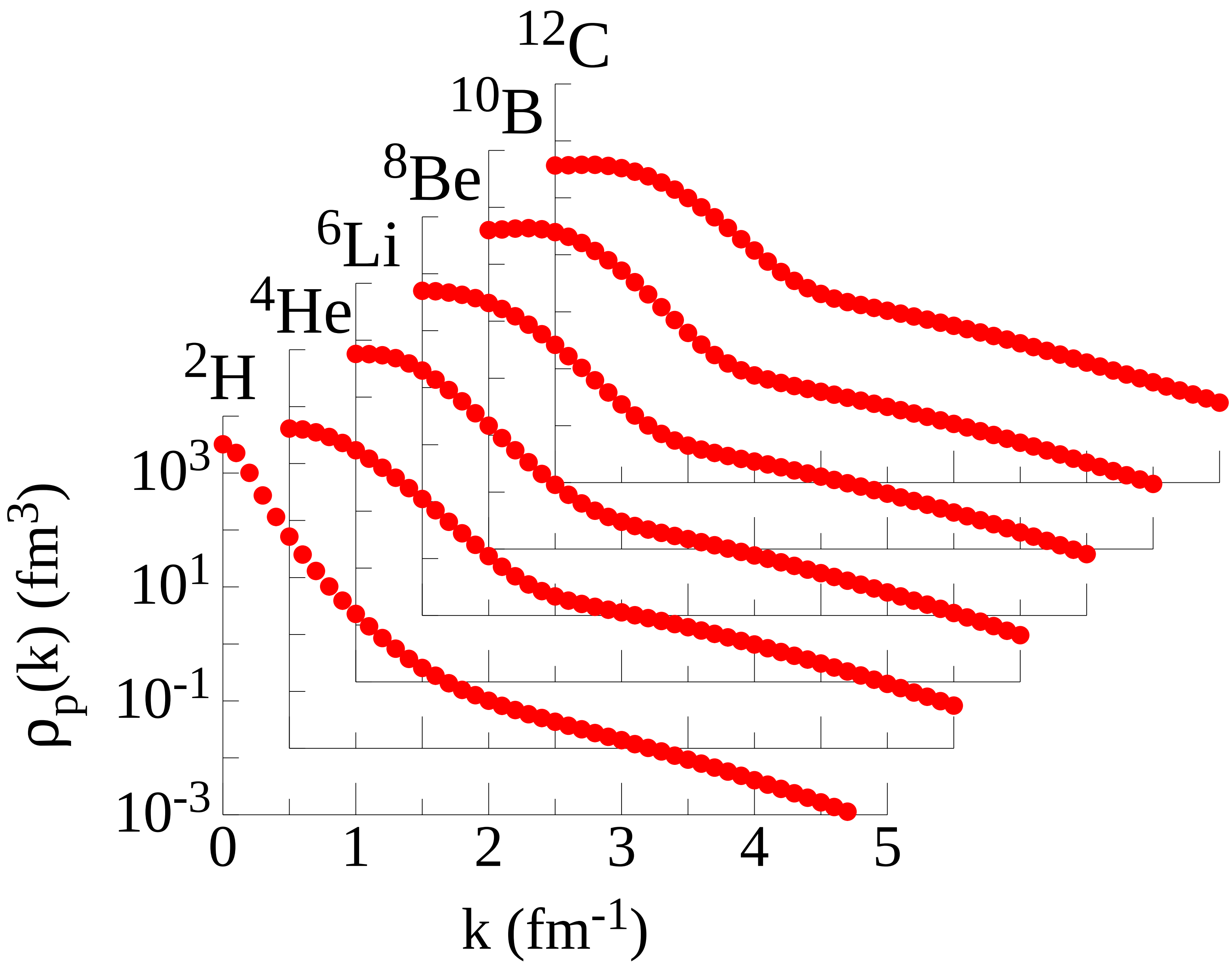

# Nucleon-Pair Momentum Distributions

Probability of finding two nucleons in a nucleus with relative momentum $\mathbf{q} = (\mathbf{q}_1 - \mathbf{q}_2)/2$ and total center-of-mass momenta $\mathbf{Q} = (\mathbf{q}_1 + \mathbf{q}_2)$ in a given spin-isospin state:

$$\rho_{ST}(\mathbf{q}, \mathbf{Q}) = \int d\mathbf{r}'_1 d\mathbf{r}_1 d\mathbf{r}'_2 d\mathbf{r}_2 d\mathbf{r}_3 \cdots d\mathbf{r}_A \, \psi^\dagger_{JM_J}(\mathbf{r}'_1, \mathbf{r}'_2, \mathbf{r}_3, \ldots, \mathbf{r}_A) \, e^{-i\mathbf{q}\cdot(\mathbf{r}_{12} - \mathbf{r}'_{12})}$$

$$e^{-i\mathbf{Q}\cdot(\mathbf{R}_{12} - \mathbf{R}'_{12})} \, P_{ST}(12) \, \psi_{JM_J}(\mathbf{r}_1, \mathbf{r}_2, \mathbf{r}_3, \ldots, \mathbf{r}_A)$$

where $P_{ST}$ is a pair spin-isospin projection operator and the normalization is:

$$N_{ST} = \int \frac{d\mathbf{q}}{(2\pi)^3} \frac{d\mathbf{Q}}{(2\pi)^3} \rho_{ST}(\mathbf{q}, \mathbf{Q})$$

and $N_{ST}$ is the total number of nucleon pairs with given spin-isospin.

This double Fourier transform is evaluated by a double Gauss-Legendre integration over each pair of nucleons in each configuration sampled by the variational Monte Carlo wave function. The angle between $\mathbf{q}$ and $\mathbf{Q}$ can be randomly chosen or at a fixed angle, such as $\mathbf{q}||\mathbf{Q}$.

The nucleon-pair momentum distribution can be projected in various ways. Here is $\rho_{ST}$, as a function of $q$, integrated over all $Q$, with projection into states of total $S$=0,1 and $T$=0,1
In an independent-pair model, $^4$He would have 3 pairs each of $ST$=10 and 01, but tensor forces shift $^1/_2$ pair of $ST$=01 to 11.

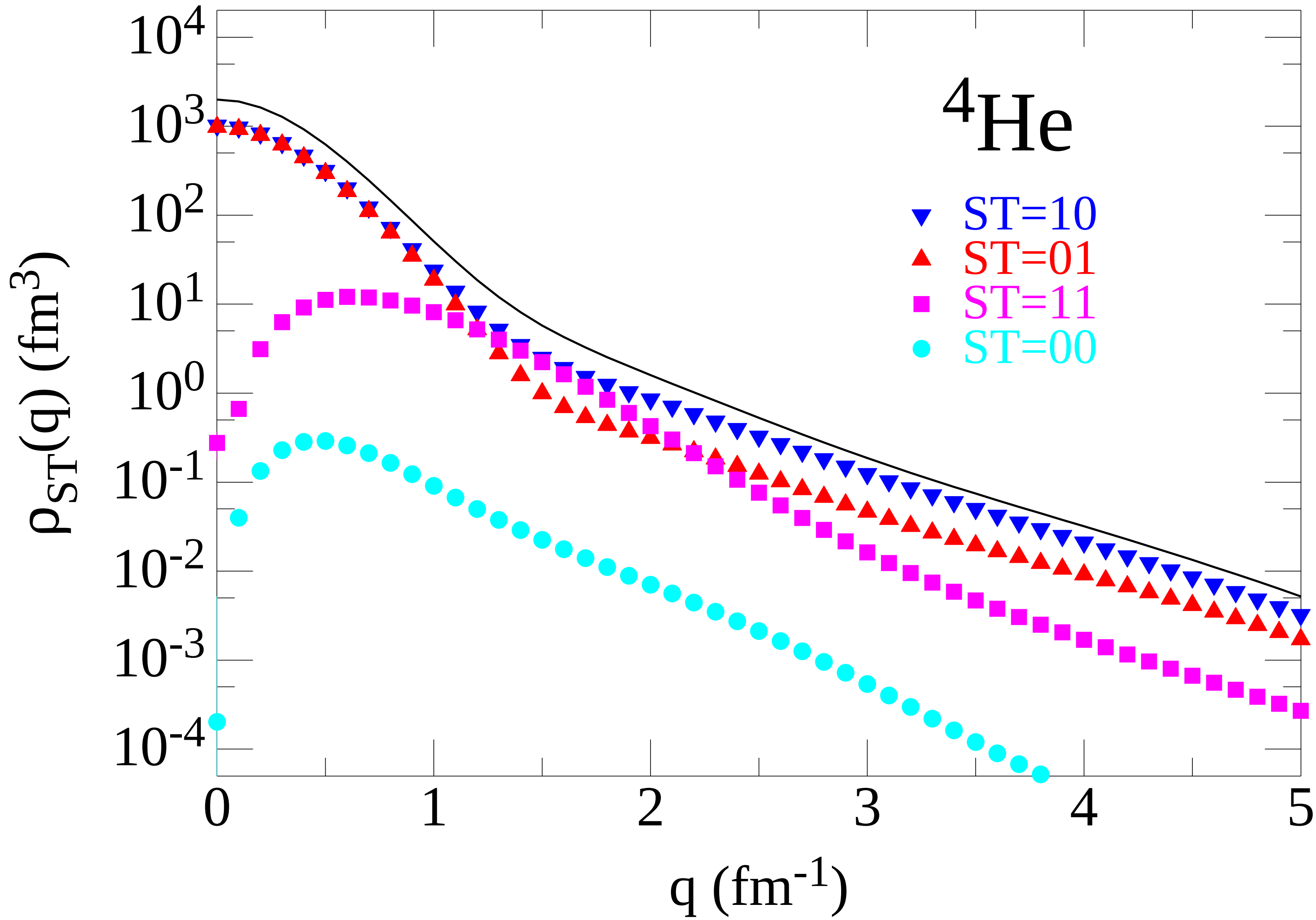

Here is $\rho_{12}$ for $^8$He, as a function of $Q$, integrated over all $q$, with projection into $nn$, $np$, and $pp$ pairs.

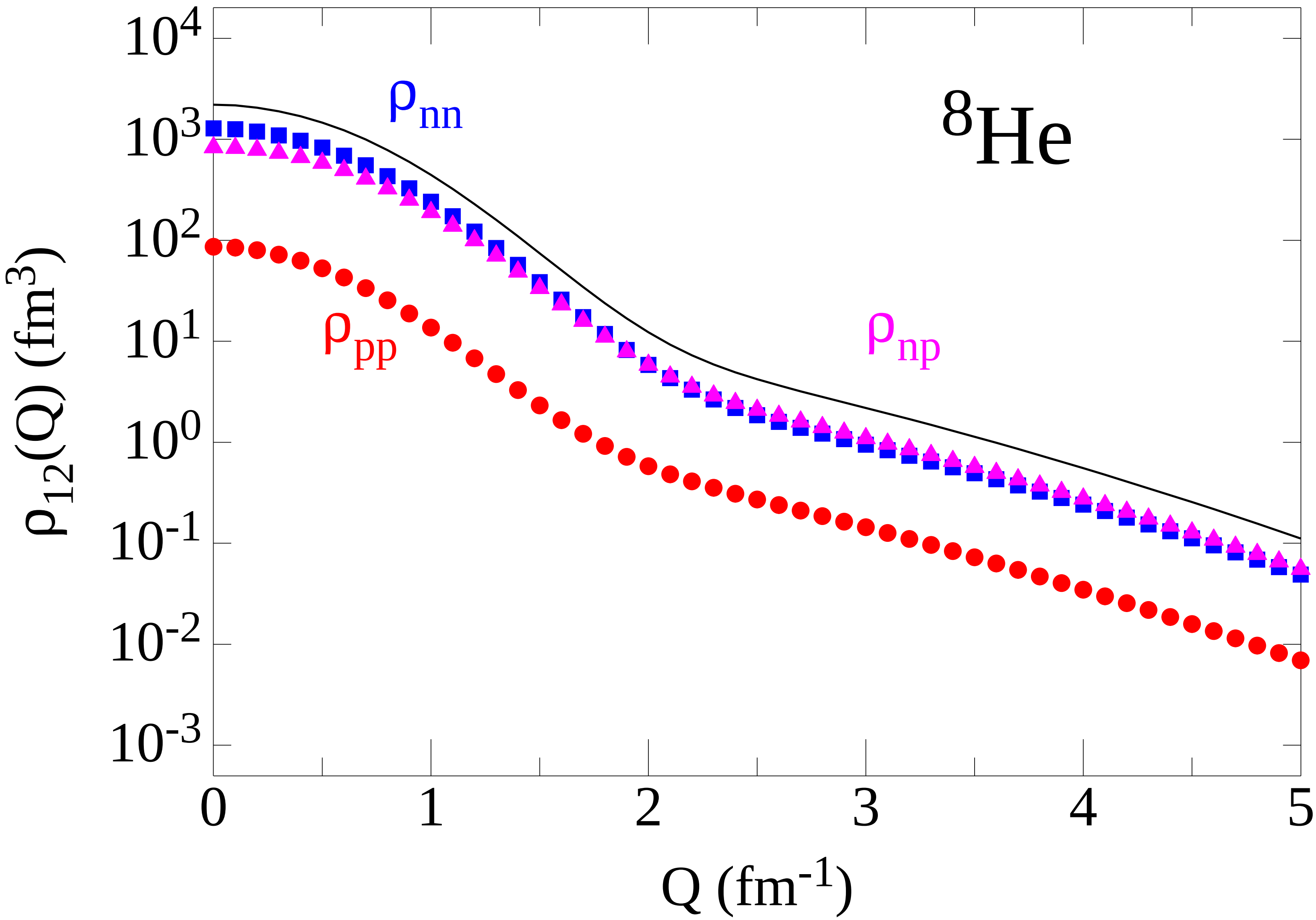

The $np$ and $pp$ momenta in $^4$He for AV18+UX averaged over all angles between **q** and **Q** shown as a function of $q$ for fixed values of $Q$. The $pp$ pairs are primarily in relative $^1S_0$ states and show a typical $S$-wave node at $Q = 0$, filled in as $Q$ increases; $np$ pairs have no node.

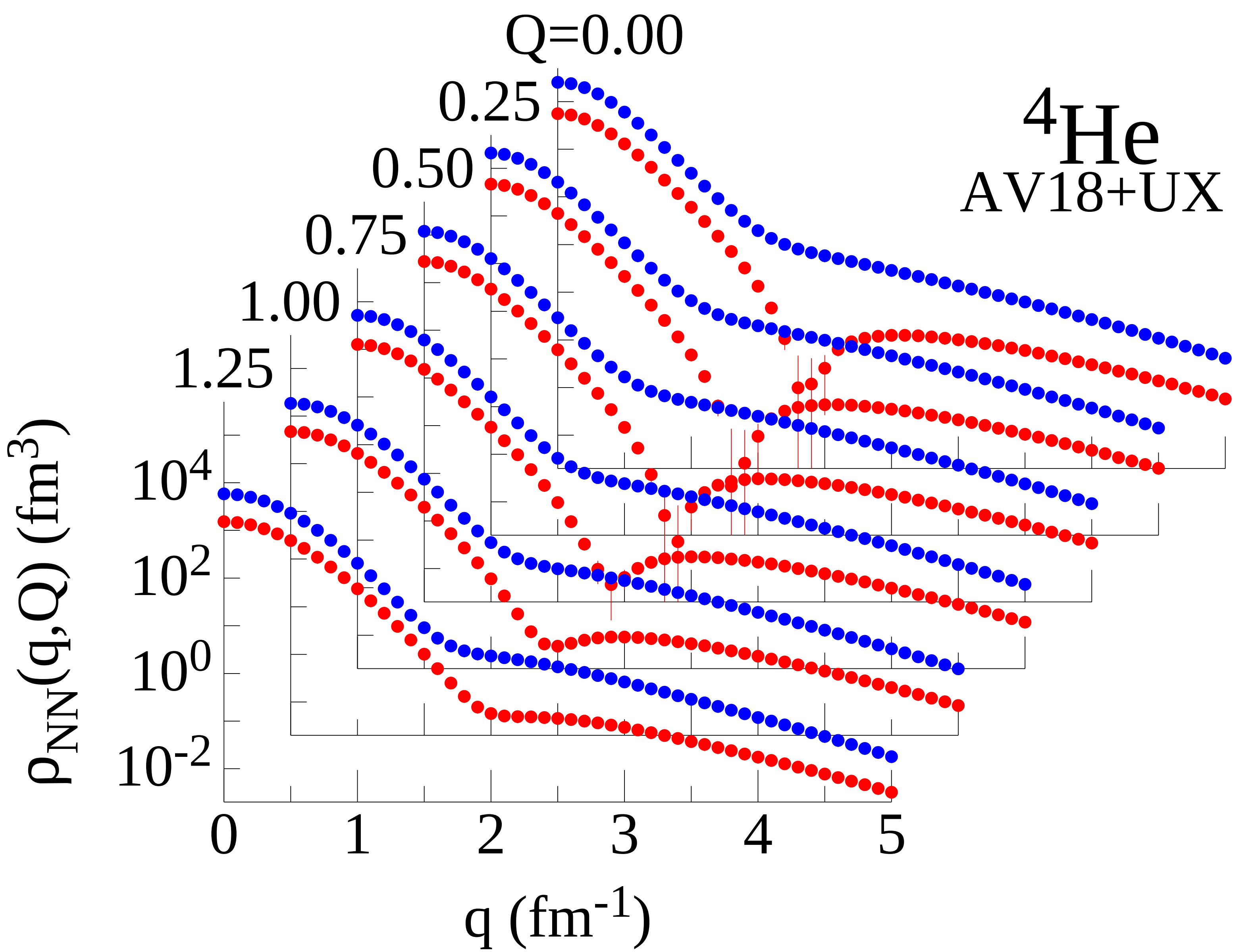

The $np$ and $pp$ momenta in $^4$He for NV2+3-Ia averaged over all angles between $\mathbf{q}$ and $\mathbf{Q}$ shown as a function of $q$ for fixed values of $Q$. The $pp$ minimum is again present although not as sharp, and both $pp$ and $np$ fall off more rapidly at high $q$.

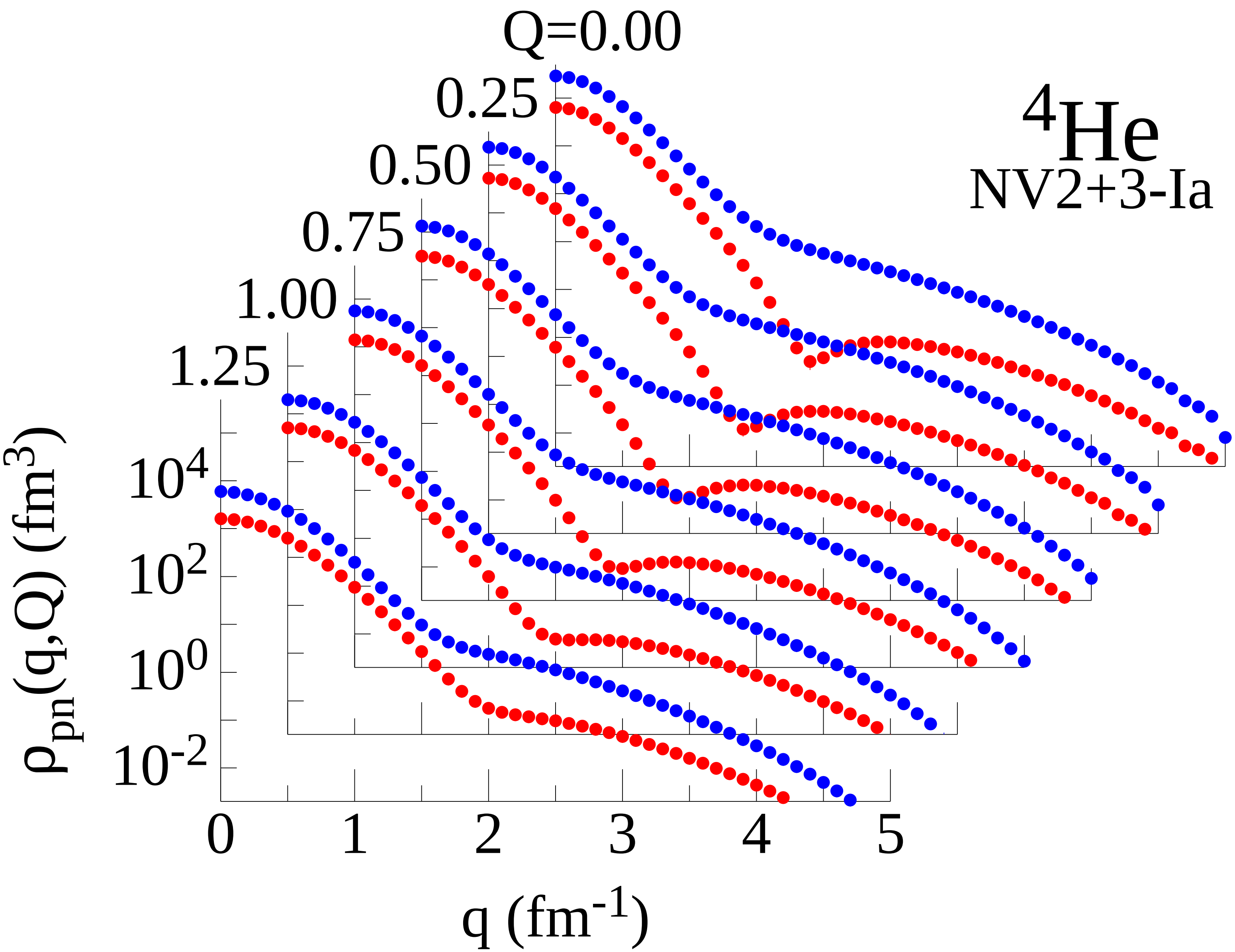

The $np$ and $pp$ momenta in $^6$Li for AV18+UX averaged over all angles between **q** and **Q**. The $pp$ minimum is softer than in $^4$He, and both $pp$ and $np$ are flatter at small $q$, but overall trend is the same.

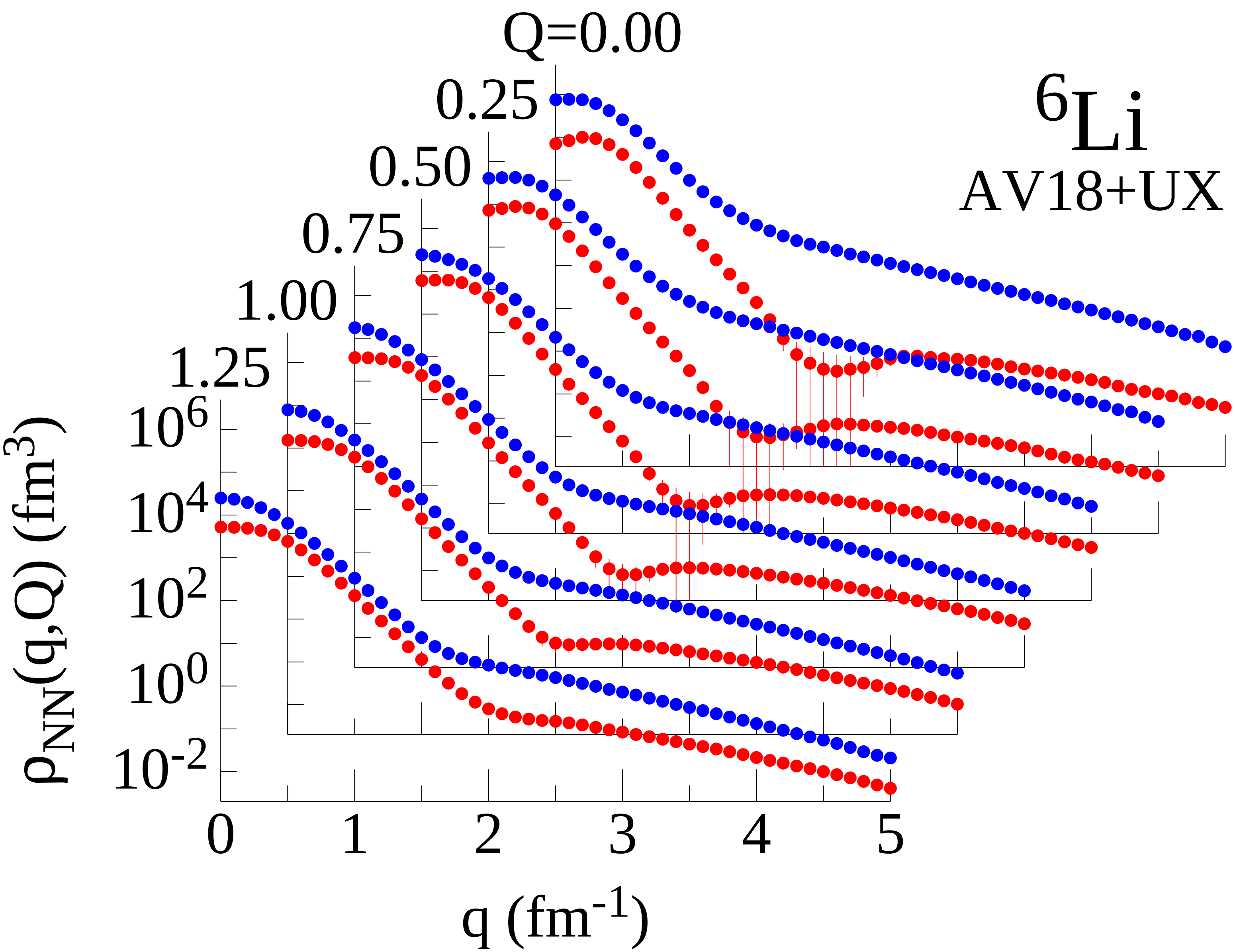

The $np$ and $pp$ momenta in $^8$Be for AV18+UX averaged over all angles between **q** and **Q**. The $pp$ minimum is still softer than in $^6$Li, and both $pp$ and $np$ are flatter at small $q$, but again overall trend is the same.

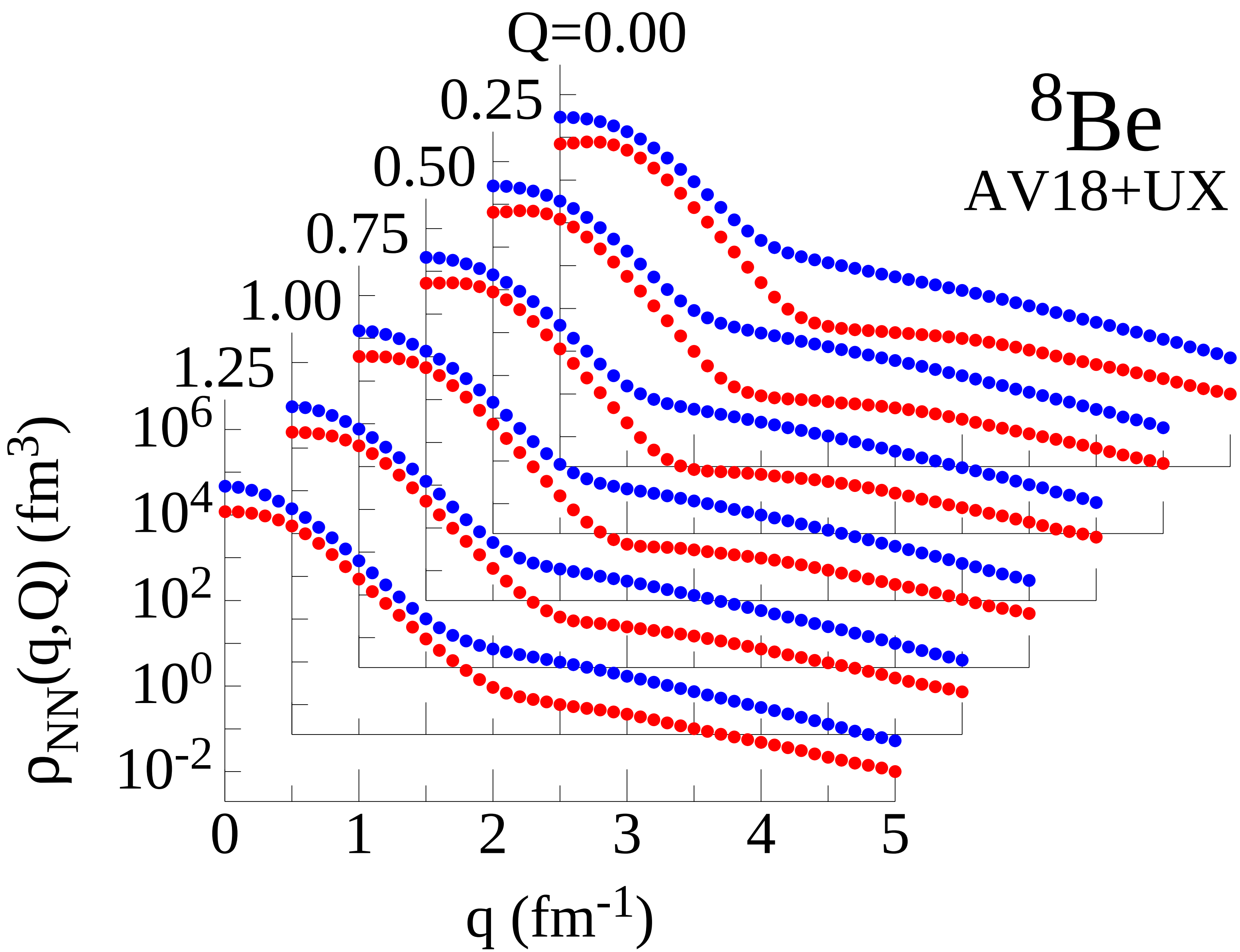

# Tabulations

Single-nucleon momentum distributions are available for many additional cases, including $^{3}$H, $^{8}$He, $^{8}$Li, $^{9}$Li, $^{9}$Be, $^{10}$Be, $^{10}$B, $^{11}$B and two-nucleon distributions for $^{3}$He
Results of CVMC calculations for $^{16}$O and $^{40}$Ca are also posted.

For anyone who wishes to use these momentum distributions, they are available on-line:

For single-nucleon momentum distributions: www.phy.anl.gov/theory/research/momenta

(single-nucleon density distributions are at www.phy.anl.gov/theory/research/density)

For two-nucleon momentum distributions: www.phy.anl.gov/theory/research/momenta2

More calculations will be posted as they become available; requests will be entertained.